Accepted manuscript (author version)

To appear in: **Majlesi Journal of Electrical Engineering (MJEE)**

Online ISSN: 2345-377X **Print ISSN:** 2345-3796

This PDF file is not the final version of the record. This version will undergo further copyediting, typesetting, and production review before being published in its definitive form. We are sharing this version to provide early access to the article. Please be aware that errors that could impact the content may be identified during the production process, and all legal disclaimers applicable to the journal remain valid.

Received: 06-Nov-2024

Revised: 18-Feb-2025

Accepted: 15-May-2025

Accepted Manuscript: Author Version

This article has license CC BY 4.0 https://creativecommons.org/licenses/by/4.0/

Accepted manuscript (author version)

DOI: 10.57647/mjee.2026.2002.10

Original Research

Hexagonal Microstrip MIMO Antenna with Defected Ground Structures for ISM/IoT Application

Farzaneh Talebi, Pejman Rezaei*, Sina Kiani

Electrical and Computer Engineering Faculty, Semnan University, Semnan, Iran.

Email: prezaei@semnan.ac.ir (Corresponding author)

Orcid: 0000-0002-1266-3229

Email: farzaneh_talebi@semnan.ac.ir

Email: sina.kiani@semnan.ac.ir

© Author(s) 2025

Abstract

In this manuscript, an original multiple-input multiple-output (MIMO) array antenna is proposed. The proposed array consists of two mirror-image elements placed adjacently. The proposed MIMO antenna is designed on the Rogers 4003C substrate with dimensions of 54 × 26 × 0.508 mm^3. The recommended MIMO antenna exhibits a fractional impedance bandwidth of 13.79% (5.4-6.2 GHz), and achieves an element isolation greater than 22 dB. The proposed MIMO array demonstrates a gain of 5 dB with an efficiency of 95% at 5.8 GHz. Additionally, the MIMO array has a channel capacity loss less of than 0.2 b/s/Hz, an envelope correlation coefficient of ≤ 0.02, a diversity gains of ≥ 9.96 dB, and a mean effective gain ratio between elements of 1 dB. Due to its optimal operating frequency, high efficiency, and compact size, this antenna is an appropriate candidate for ISM/IoT applications.

Keywords: Decoupling network; Defected ground structure; ISM/IoT applications; Microstrip MIMO antenna; Mutual coupling.

1. Introduction

In recent years, wireless communications have witnessed significant revolutionary advancements. The field of wireless communication systems encompasses a wide range of topics, including the development of communication chains, waveform design, interference and traffic management, channel modeling, compensating for radio hardware imperfections, symbol and bit recovery, and the enhancement of wireless security [1-3]. In the era of digital communication, the widespread use of platforms among new generations necessitates those wireless systems provide the highest data transmission rates, robust connectivity, enhanced reliability, and strong security measures [4, 5]. In recent years, MIMO antennas have obtained significant attention in non-line-of-sight wireless communications because they can utilize multiple paths for transmitting and receiving signals [6, 7]. MIMO antennas are commonly used to enhance reliability and increase data rates, thereby reducing interference from other wireless devices [8]. MIMO antennas are suitable for communication systems like LTE and Wi-Fi [9].

One challenge of MIMO antennas is the need to decrease mutual coupling between elements. When designing MIMO antennas, this parameter must be significantly reduced to ensure each antenna operates independently and efficiently [10, 11]. Some methods for controlling mutual coupling include decoupling networks, split-ring resonators (SRRs), complementary split-ring resonators (CSRRs), varactor diodes, and electromagnetic bandgap structures [12, 13].

Varactor diodes are integrated tuning components that help control frequency and radiation patterns. They utilize a dielectric material, which enhances isolation. However, incorporating varactor diodes can increase complexity, reduce overall efficiency, and require high voltage toggling between the ON and OFF states [14].

Accepted Manuscript: Author Version

This article has license CC BY 4.0 https://creativecommons.org/licenses/by/4.0/

Accepted manuscript (author version)

Split Ring Resonators (SRRs) enhance antenna performance by creating a resonant effect for precise frequency calibration. Complementary Split-Ring Resonators (CSRRs) are essentially the inverse of SRRs; they provide high isolation between closely spaced antennas, reduce mutual coupling, and improve the efficiency of Multiple Input Multiple Output (MIMO) systems. However, the resonant frequency of these components is sensitive to external conditions, and there can be challenges in their design and fabrication [15, 16].

Another method for reducing mutual coupling is the use of defected ground structures (DGS). DGSs have been applied in various communication devices, such as antennas [17, 18], planar waveguides [19], sensors [20-22], filters [23, 24], oscillators [25], and biosensors [26-28], to enhance performance. In recent years, antenna designers have been focused on developing wideband and wearable antennas, particularly for MIMO antenna [29-31]. Consequently, substantial research has been conducted in the areas of reconfigurable and wearable MIMO antennas [32], as well as UWB MIMO [32], positioning them as promising options for next-generation antennas [34, 35].

In this paper, an innovative MIMO microstrip array antenna is presented. The proposed antenna consists of two incomplete hexagonal patches, both of which are fed by a 50 Ω microstrip line. The antenna is placed on the Rogers 4003C board, with a thickness of 0.508 mm, a relative permittivity of 3.38, and a loss tangent of 0.0027. The primary challenge in MIMO antennas is achieving sufficient isolation between the antenna elements. This paper discusses a solution where the antenna elements are positioned on a defected ground structure (DGS) to minimize mutual coupling while maintaining a compact dimension [36]. Consequently, the proposed MIMO antenna operates within the frequency range of 5.4-6.2 GHz. It offers high isolation, a compact design, and low cost, making it well-suited for Internet of Things and Industrial, Scientific, and Medical (ISM/IOT) applications.

Section 2 discusses the planning steps for a single microstrip antenna, including an analysis of the S11 parameters at each stage, with surface current measurements taken at 5.8 GHz. Section 3 presents the designed sample and the constructed prototype of the proposed MIMO antenna, illustrated with S-parameters and radiation patterns. Finally, Section 4 details the obtained results.

2. Designing Steps of Single Microstrip Element

The modified microstrip antenna is illustrated in Figure 1. The Rogers 4003C substrate is utilized due to its low cost, robustness, and availability. The initial step in designing a single microstrip antenna is to determine the patch parameters using equations (1-5) [37]. This research utilizes the DGS to improve isolation by altering the return path of surface current at the operating frequency, based on previous studies conducted by [38], [39], [40], and [41]. The second step involves optimizing the antenna gain by loading slot on the patch, allowing the surface current to meander while maintaining the dimensions. In the third step, a slot is added to the patch, redirecting the surface current along the patch. Consequently, this increases the bandwidth and shifts the resonance frequency closer to 5.8 GHz, optimizing the antenna for ISM/IoT applications. The final goal of this article is to design a MIMO antenna. Therefore, the ground structure is modified to enhance isolation, gain, and efficiency. Figure 2 presents the design evolution of the single-element microstrip antenna, which features a defective ground structure. It includes an analysis of the S-parameter diagram and the variations in resonant frequencies. Additionally, the simulated far-field radiation pattern and gain of the single-element antenna is 3.42 dB at 5.8 GHz. Furthermore, Figure 3 illustrates the surface current distributions for the single-element antenna for both the (top/bottom layer) at a frequency of 5.8 GHz.

$$W = \frac{c}{2f_r}\sqrt{\frac{2}{\varepsilon_r+1}} \tag{1}$$

Where c is the velocity of light, f_r is the resonant frequency and ε_r is the dielectric constant of substrate.

$$L = L_{eff} - \Delta L \tag{2}$$

Where L_{eff} is effective length of the patch given as follows:

$$L_{eff} = \frac{c}{2f_r\sqrt{\varepsilon_{eff}}} \tag{3}$$

And ΔL is the extended incremental length given as follows:

$$\Delta L = 0.412h\frac{(\varepsilon_{eff}+0.3)\left(\frac{w}{h}+0.264\right)}{(\varepsilon_{eff}-0.258)\left(\frac{w}{h}+0.8\right)} \tag{4}$$

Where ε_{eff} is the effective dielectric constant given as follows:

This article has license CC BY 4.0 https://creativecommons.org/licenses/by/4.0/

$$\varepsilon_{eff} = \frac{\varepsilon_r+1}{w} + \frac{\varepsilon_r-1}{w}(1+\frac{12h}{w})^{-\frac{1}{2}} \quad (5)$$

Table 1 presents the calculated dimensions of the proposed patch antenna, which were derived using equations (1-5). These dimensions have been adjusted using CST Microwave Studio to improve the overall performance of the antenna for operation at 5.8 GHz, as illustrated in Figure 1.

Table 1.

Fig. 1.

Fig. 2.

Fig. 3.

3. Analysis Results of Microstrip MIMO Array

The designed and fabricated sample of the top/bottom of a proposed MIMO structure is presented in Figures 4 and 5, respectively, which consists of double microstrip antennas arranged next to one another in a mirror pattern.

Fig. 4.

Fig. 5.

According to Figures 6a, b, the bandwidth of this MIMO antenna obtained 13.79% (5.4-6.2 GHz), and isolation is more than 22 dB (S21 ≤ -22 dB), which caused optimal performance.

Fig. 6.

The photograph of the manufactured MIMO antenna prototype in the anechoic chamber is presented in Figure 7. Figures 8a and b are the simulated radiation patterns on the H-plane and E-plane of the proposed microstrip MIMO radiator at 5.8 GHz. The peak gain and efficiency have obtained 5dB and 95%, respectively. The overall simulation and measurement outcomes of the MIMO array have an appropriate overlap, however, due to the fabrication faults and different conditions, some mismatches have occurred between results. Figures 8c and d, and 8e and f demonstrate simulated radiation patterns on both the H-plane and E-plane of the proposed microstrip MIMO far-field pattern at 5.4 GHz and 6.2 GHz. Figure 8d presents the antenna gain over its operational frequency range. According to the data, the antenna gains at 5.2, 5.8, and 6.2 GHz are 4.9, 5, and 4.8 dB, respectively. In the MIMO configuration, the ground planes of the antenna elements are merged and expanded to create a unified structure. Consequently, it is expected that the radiation pattern shown in Figure 8b will exhibit slight differences compared to the single-element case presented in Figure 2f.

Fig. 7.

Fig. 8.

3.1. MIMO Specifications

To legitimize the proposed antenna specifications as a MIMO antenna, numerous parameters for example channel capacity reduction (CCL), mean effective gain (MEG), envelope correlation coefficient (ECC), and diversity gain (DG) should be considered. All the MIMO antenna parameters have been investigated according to the S-parameters.

3.2. ECC and DG Parameters

ECC can estimate the correlation and isolation between MIMO antenna elements [42]. According to the third-generation partnership project (3GPP) industrial standard, to keep an optimal implementation of a MIMO antenna, the ECC value is necessary to be below 0.5, so that each element antenna can function independently, without affecting another element [43]. The simulated and measured ECC is calculated using Equation (6), with scattering

Accepted manuscript: Author Version

This article has license CC BY 4.0 https://creativecommons.org/licenses/by/4.0/

parameter values [13]. Figure 9a illustrates ECC, which is below 0.02 for all 5.4-6.2 GHz bandwidth.

$$\mathrm{ECC} = \frac{|S_{11}^{*}S_{12}+S_{21}^{*}S_{22}|}{(1-|S_{11}|^{2}-|S_{21}|^{2})(1-|S_{22}|^{2}-|S_{12}|^{2})} \quad (6)$$

In the MIMO antenna, diversity gain describes the obtained gain from multiple antennas in comparison to the singular element. Regularly a DG standard must be about 10 dB [44]. According to Equation (7), the ECC of a MIMO array can be used to determine DG [45]. Figure 9a shows that DG is close to 10 dB over the operating range.

$$\mathrm{DG} = 10\sqrt{1-\mathrm{ECC}^{2}} \quad (7)$$

3.3. CCL Parameter

Channel capacity can be expressed based on Shannon's theorem, which is an extreme possible information transfer rate through a communication channel without any interference. As a result, the system performance decline can be measured in CCL terms. The acceptable CCL values for MIMO systems are lower than 0.4 b/s/Hz. The CCL results are presented in Figure 9b, which are below 0.2 b/s/Hz for the entire operational bandwidth. The CCL can be explained by Equation (8), where β^{R} is an antenna correlation matrix [46, 47]:

$$\mathrm{CCL(LOSS)} = -\log_{2}\det(\beta^{R}) \quad (8)$$

Where:

$$\beta^{R} = \begin{bmatrix} R_{ii} & R_{ij} \\ R_{ji} & R_{jj} \end{bmatrix} \quad (9)$$

$$R_{ii} = 1-\left(|s_{ii}|^{2}+|s_{ij}|^{2}\right) \quad (10)$$

$$R_{ij} = -\left(S_{ii}^{*}S_{ij} + S_{ji}^{*}S_{jj}\right) \quad (11)$$

3.4. MEG Parameter

In the MIMO antenna with multipath fading situation, MEG compares the power that is given by a multiple antenna to an isotropic antenna obtained power. Matching power level, the ratio between MEGs (MEG1/ MEG2) ought to be less than 3 dB [48]. Figure 9c shows the ratio between MEGs which is 1dB, within the standard range. MEGs can be estimated using Equations (12) and (13), where $\eta_{1,rad}$ and $\eta_{2,rad}$ are the radiation coefficients in port 1 and 2, which are calculated by S-parameters for MEG1 and MEG2, respectively [49]:

$$\mathrm{MEG}_{1} = 0.5\eta_{1,\mathrm{rad}} = 0.5\left[1-|S_{11}|^{2}-|S_{12}|^{2}\right] \quad (12)$$

$$\mathrm{MEG}_{2} = 0.5\eta_{2,\mathrm{rad}} = 0.5\left[1-|S_{12}|^{2}-|S_{22}|^{2}\right] \quad (13)$$

Fig. 9.

The IoT is a vast integrated network that enables the exchange of large amounts of data at high speeds. IoT is recognized for its affordability, intermediate data rates, and an operating frequency range between 100 MHz and 5.8 GHz. IoT applications do not require specific bandwidth when operating at a frequency of 5.8 GHz [50]. The ISM band technology is primarily utilized in various applications. One of the frequency ranges available for ISM applications is 5.725 to 5.875 GHz [51, 52]. Therefore, the proposed antenna operating within a frequency range of 5.8 to 6.2 GHz with high gain and efficiency is suitable for ISM and IoT applications.

Table 2

Table 2 presents a comparison of the proposed MIMO antenna with results from similar studies. The analysis reveals that the proposed antenna exhibits excellent efficiency when compared to references [54], [67], and [69]. It also demonstrates good gain relative to [42], [63], and [65]. Furthermore, in terms of isolation, it is comparable to studies [11], [66], and [68]. Consequently, the proposed MIMO antenna stands out as a suitable option for ISM/IoT applications due to its compact size, impressive gain, and high efficiency.

4. Conclusions

This study presents an original 2 × 1 microstrip MIMO array antenna for frequencies range between 5.4 GHz

Accepted Manuscript: Author Version

This article has license CC BY 4.0 https://creativecommons.org/licenses/by/4.0/

and 6.2 GHz, achieving a fractional bandwidth of 13.79%. The planned MIMO array is constructed with double mirror elements on a Rogers 4003C board, with dimensions of 54 × 26 × 0.508 mm³. The outcomes of the proposed antenna demonstrate a peak gain of 5 dB and an efficiency of 95% at 5.8 GHz frequency. Additionally, the specifications of this design have been compared with various similar works. According to these comparisons, this antenna is appropriate for ISM/IoT applications.

Acknowledgment

This research is funded by Semnan University, research grant 1403942. The authors would like to thank all the members of antenna laboratory at Iran Telecommunication Research Center (ITRC), for their cooperation. Also, the authors would like to thank the Editor and reviewers for their constructive comments.

Data Availability. All data generated or analyzed during this study are included in this published article.

Funding. There is no funding for this work.

Conflicts of interest. The authors declare no conflict of interest.

Ethics. The authors declare that the present research work has fulfilled all relevant ethical guidelines required by COPE.

This article is licensed under a Creative Commons Attribution 4.0 International License.

©The Author(s) 2024

References

[1] M. M. Fakharian, M. Alibakhshikenari, C. H. See, and R. Abd-Alhameed, "A high gain multiband offset MIMO antenna based on a planar log-periodic array for Ku/K-band applications," Sci. Rep., vol. 12, no. 1, p. 4044, 2022. doi: 10.1038/s41598-022-07866-1.

[2] A. Khatami, J. Meiguni, A. AmneElahi, et al., "Compact via-coupling fed monopulse antenna with orthogonal tracking capability in radiation pattern," IEEE Antennas Wirel. Propag. Lett., vol. 19, no. 8, pp. 1443–1446, 2020. doi: 10.1109/LAWP.2020.3005023.

[3] J. C. Dash and D. Sarkar, "Microstrip patch antenna system with enhanced inter-port isolation for full-duplex/MIMO applications," IEEE Access, vol. 9, pp. 156222–156228, 2021.

[4] S. Kiani, P. Rezaei, and M. Fakhr, "On-chip coronavirus shape antenna for wide band applications in terahertz band," J. Opt., vol. 52, no. 2, pp. 860–867, 2023. doi: 10.1007/s12596-022-01048-y.

[5] S. Kiani, P. Rezaei, and M. Khajenoori, "Wideband sun-star shape coplanar waveguide antenna for terahertz sensing applications," Results Opt., vol. 19, p. 100815, 2025. doi: 10.1016/j.rio.2025.100815.

[6] P. Sharma, R. N. Tiwari, P. Singh, et al., "MIMO antennas: Design approaches, techniques and applications," Sensors, vol. 22, no. 20, p. 7813, 2022. doi: 10.3390/s22207813.

[7] Z. Niu, H. Zhang, Q. Chen, and T. Zhong, "Isolation enhancement for 1×3 closely spaced E-plane patch antenna array using defect ground structure and metal-vias," IEEE Access, vol. 7, pp. 119375–119383, 2019. doi: 10.1109/ACCESS.2019.2937385.

[8] B. Bayarzaya, N. Hussain, W. A. Awan, et al., "A compact MIMO antenna with improved isolation for ISM, sub-6 GHz, and WLAN application," Micromachines, vol. 13, no. 8, p. 1355, 2022. doi: 10.3390/mi13081355.

[9] M. Y. Jamal, M. Li, and K. L. Yeung, "Isolation enhancement of closely packed dual circularly polarized MIMO antenna using hybrid technique," IEEE Access, vol. 8, pp. 11241–11247, 2020. doi: 10.1109/ACCESS.2020.2964902.

[10] E. Atashpanjeh and P. Rezaei, "Innovative design for mutual coupling reduction in dual-element array antennas for ISM applications using whale optimization algorithm," Prog. Electromagn. Res. C, vol. 152, pp. 121–129, 2025. doi: 10.2528/PIERC24122203.

[11] A. Omidvar, P. Rezaei, and E. Atashpanjeh, "Mutual coupling reduction with Peyton Turtle pattern nearfield surface for MIMO patch antenna," Frequenz, vol. 77, no. 7–8, pp. 395–401, 2023. doi: 10.1515/freq-2022-0150.

[12] M. Alibakhshikenari, F. Babaeian, B. S. Virdee, et al., "A comprehensive survey on various decoupling mechanisms with focus on metamaterial and metasurface principles applicable to SAR and MIMO antenna systems," IEEE Access, vol. 8, pp. 192965–193004, 2020. doi: 10.1109/ACCESS.2020.3032826.

[13] A. Iqbal, A. Smida, A. J. Alazemi, et al., "Wideband circularly polarized MIMO antenna for high data wearable biotelemetric devices," IEEE Access, vol. 8, pp. 17935–17944, 2020. doi: 10.1109/ACCESS.2020.2967397.

[14] Q. H. Kareem, R. A. Shihab, and H. H. Kareem, "Compact dual-polarized reconfigurable MIMO antenna based on a varactor diode for 5G mobile terminal applications," Prog. Electromagn. Res. C, vol. 15, no. 137, pp. 185–198, 2023. doi: 10.2528/PIERC23072204.

This article has license CC BY 4.0 https://creativecommons.org/licenses/by/4.0/

[15] N. Sheriff, S. Kamal Abdul Rahim, H. Tariq Chattha, and T. Kim Geok, "Multiport single element MIMO antenna systems: A review," Sensors, vol. 23, no. 2, p. 747, 2023. doi: 10.3390/s23020747.

[16] K. Satish, T. Gunasekaran, S. A. Al Ismaili, and S. Balambigai, "MIMO-CSRR antenna for ISM band applications," Res. Square, pp. 1–10, 2021. doi: 10.21203/rs.3.rs-342965/v1.

[17] Y. Zehforoosh and M. Jalali, "A low mutual coupling four-port MIMO antenna for WiMAX, Bluetooth and WLAN," Majlesi J. Electr. Eng., vol. 18, no. 2, pp. 1–9, 2024. doi: 10.57647/j.mjee.2024.1802.27.

[18] R. Khajeh Mohammad Lou, T. Aribi, and T. Sedghi, "Quad-band multiple input multiple output modified PIFA antenna for WLAN and LTE mobile applications," Majlesi J. Electr. Eng., vol. 17, no. 2, pp. 99–108, 2023. doi: 10.30486/mjee.2023.1976700.1047.

[19] S. Kiani and P. Rezaei, "Microwave substrate integrated waveguide resonator sensor for non-invasive monitoring of blood glucose concentration: Low cost and painless tool for diabetics," Measurement, vol. 219, p. 113232, 2023. doi: 10.1016/j.measurement.2023.113232.

[20] M. Hemmati, M. Jafar Tafreshi, M. H. Ehsani, S. Alamdari, "Highly sensitive and wide-range flexible sensor based on hybrid BaWO4@CS nanocomposite," Ceramics International, vol. 48, no. 18, pp. 26508-26518, 2022, doi: 10.1016/j.ceramint.2022.05.347.

[21] S. Khani and M. Hayati, "High resolution refractive index and temperature sensor with Fano resonance in disk and parenthesis-shaped plasmonic cavities," Results Opt., vol. 19, p. 100816, 2025. doi: 10.1016/j.rio.2025.100816.

[22] M. H. Ehsani, S. Alamdari, "Biomaterials: Fundamentals, processing, and applications. In: Ikhmayies, S.J. (eds) Advances in Biomaterials Research. Advances in Material Research and Technology. Springer, 2025, doi: 10.1007/978-3-031-97481-6_1.

[23] B. Mohammadi, A. Valizade, et al., "Design of a compact dual-band-notch ultra-wideband bandpass filter based on wave cancellation method," IET Microw. Antennas Propag., vol. 9, no. 1, pp. 1–9, 2015. doi: 10.1049/iet-map.2014.0372.

[24] B. Mohammadi, A. Valizade, et al., " New design of compact dual band-notch ultra-wideband bandpass filter based on coupled wave canceller inverted T-shaped stubs," IET Microw. Antennas Propag., vol. 9, no. 1, pp. 64–72, 2015. doi: 10.1049/iet-map.2014.0484.

[25] H. N. Varcheh, P. Rezaei, and S. Kiani, "A modified Jerusalem microstrip filter and its complementary for low phase noise X-band oscillator," Int. J. Microw. Wireless Technol., vol. 15, no. 10, pp. 1707–1716, 2023. doi: 10.1017/S1759078723000703.

[26] A. H. Alipour, S. Khani, M. Ashoorirad, and R. Baghbani, "Trapped multimodal resonance in magnetic field enhancement and sensitive THz plasmon sensor for toxic materials accusation," IEEE Sens. J., vol. 23, no. 13, pp. 14057–14066, 2023. doi: 10.1109/JSEN.2023.3278321.

[27] A. R. Jalalvand, Z. Rashidi, and M. Khajenoori, "Sensitive and selective simultaneous biosensing of nandrolone and testosterone as two anabolic steroids by a novel biosensor assisted by second-order calibration," Steroids, vol. 189, p. 109138, 2023. doi: 10.1016/j.steroids.2022.109138.

[28] S. Khani and M. Hayati, "Optical biosensors using plasmonic and photonic crystal band-gap structures for the detection of basal cell cancer," Sci. Rep., vol. 12, no. 1, p. 5246, 2022. doi: 10.1038/s41598-022-09213-w.

[29] M. H. Ashouri, S. Fakhte, and M. M. Taskhiri, "A broadband high gain circularly polarized magneto-electric dipole antenna with chiral metamaterial for 5G/WIMAX wireless network," Wireless Netw., vol. 30, pp. 845–855, 2024. doi: 10.1007/s11276-023-03529-9.

[30] K. Ramasamy, B. A. Sapna, and M. Jayasheela, "A novel wearable monopole antenna with controlled SAR using metamaterial," Int. J. Microw. Wireles Technol., vol. 15, no. 9, pp. 1524–1536, 2023. doi: 10.1007/s11276-023-03529-9.

[31] S. Fakhte and M. H. Ashouri, "Broadband half mode substrate integrated waveguide H-plane horn antenna," Majlesi J. Electr. Eng., vol. 17, no. 2, pp. 23–28, 2023. doi: 10.30486/mjee.2023.1970195.0.

[32] Z. Lu, H. Lin, Z. Wang, W. Nie, and W. Mu, "Compact ACS-fed MIMO antenna with dual-band notch characteristics for UWB applications," Int. J. Microw. Wireless Technol., vol. 16, no. 3, pp. 478–486, 2024. doi: 10.1017/S1759078723001277.

[33] A. A. Ibrahim, A. Eltokhy, and A. F. Daw, "Four ports MIMO printed antenna with high isolation for UWB and X-band systems," Int. J. Microw. Wireless Technol., vol. 15, no. 9, pp. 1601–1609, 2023. doi: 10.1017/S1759078723000296.

[34] M. Borhani Kakhki and P. Rezaei, "Reconfigurable microstrip slot antenna with DGS for UWB applications," Int. J. Microw. Wireless Technol., vol. 9, no. 7, pp. 1517–1522, 2017. doi: 10.1017/S1759078717000034.

[35] M. H. Ashouri and S. Fakhte, "Reduction of mutual coupling between two circularly polarized magneto-electric dipole antennas using metasurface wall polarization converter for 5G application," Majlesi J. Electr. Eng., vol. 18, no. 1, pp. 55–63, 2024. doi: 10.30486/mjee.2023.1991539.1180.

[36] C. Güler and S. E. Bayer Keskin, "A novel high isolation 4-port compact MIMO antenna with DGS for 5G applications," Micromachines, vol. 14, no. 7, p. 1309, 2023. doi: 10.3390/mi14071309.

[37] J. Colaco and R. Lohani, "Design and Implementation of microstrip patch antenna for 5G applications," in 5th Int. Conf. Commun. Electron. Syst. (ICCES), Jun. 2020, pp. 682–685. doi: 10.1109/ICCES48766.2020.9137921.

[38] E. Ez-Zaki, H. Belahrach, A. Ghammaz, S. Ahmad, et al., "Double negative (DNG) metamaterial-based Koch fractal MIMO antenna design for sub-6-GHz V2X communication," IEEE Access, vol. 11, pp. 77620–77635, 2023, doi: 10.1109/ACCESS.2023.3296599.

[39] D. Rusdiyanto, M. Muslim, D. W. Astuti, Y. G. Adhiyoga, and C. Apriono, "The design of microstrip antenna using DGS and series parasitic methods for C-band applications in satellite communications," J. Informatics Telecommun. Eng., vol. 8, no. 2, pp. 303–312, 2025, doi: 10.31289/jite.v8i2.12695.

Accepted Manuscript Author Version

This article has license CC BY 4.0 https://creativecommons.org/licenses/by/4.0/

[40] P. Singh, "Design and analysis of compact MIMO antenna for UWB applications with reduced mutual coupling," Authorea Preprints, pp. 1–10, 2024, doi: 10.36227/techrxiv.173014736.66446743/v1.
[41] S. Thiruvenkadam, E. Parthasarathy, S. K. Palaniswamy, S. Kumar, and L. Wang, "Design and performance analysis of a compact planar MIMO antenna for IoT applications," Sensors, vol. 21, no. 23, p. 7909, 2021, doi: 10.3390/s21237909.
[42] J. Kulkarni, A. Desai, and C. Y. D. Sim, "Two port CPW-fed MIMO antenna with wide bandwidth and high isolation for future wireless applications," Int. J. RF Microw. Comput.-Aided Eng., vol. 31, no. 8, e22700, 2021, doi: 10.1002/mmce.22700.
[43] A. K. Dwivedi, A. Sharma, A. K. Pandey, and V. Singh, "Two port circularly polarized MIMO antenna design and investigation for 5G communication systems," Wireless Pers. Commun., vol. 120, no. 3, pp. 2085–2099, 2021, doi: 10.1007/s11277-021-08461-9.
[44] G. Saxena, P. Jain, and Y. K. Awasthi, "High diversity gain super-wideband single band-notch MIMO antenna for multiple wireless applications," IET Microw. Antennas Propag., vol. 14, no. 1, pp. 109–119, 2020, doi: 10.1049/iet-map.2019.0450.
[45] Y. Cheng, H. Liu, B. Q. Sheng, and L. Zhu, "A compact 4-element MIMO antenna for terminal devices," Microw. Opt. Technol. Lett., vol. 62, no. 9, pp. 2930–2937, 2020, doi: 10.1002/mop.32396.
[46] N. Kumar and R. Khanna, "A two element MIMO antenna for sub-6 GHz and mmWave 5G systems using characteristics mode analysis," Microw. Opt. Technol. Lett., vol. 63, no. 2, pp. 587–595, 2021, doi: 10.1002/mop.32626.
[47] S. Kumar, D. Nandan, K. Srivastava, S. Kumar, H. Singh, M. Marey, and B. K. Kanaujia, "Wideband circularly polarized textile MIMO antenna for wearable applications," IEEE Access, vol. 9, pp. 108601–108613, 2021, doi: 10.1109/ACCESS.2021.3101441.
[48] G. Das, A. Sharma, and R. K. Gangwar, "Dielectric resonator based circularly polarized MIMO antenna with polarization diversity," Microw. Opt. Technol. Lett., vol. 60, no. 3, pp. 685–693, 2018, doi: 10.1002/mop.31033.
[49] J. Kulkarni, R. K. Gangwar, and J. Anguera, "Broadband and compact circularly polarized MIMO antenna with concentric rings and oval slots for 5G application," IEEE Access, vol. 10, pp. 29925–29936, 2022, doi: 10.1109/ACCESS.2022.3157914.
[50] A. A. Elijah and M. Mokayef, "Miniature microstrip antenna for IoT application," Mater. Today: Proc., vol. 29, pp. 43–47, 2020, doi: 10.1016/j.matpr.2020.05.678.
[51] M. R. Samy and A. Gudipalli, "Design circular polarized antenna at ISM band for WBAN using parasitic elements," Heliyon, vol. 10, no. 6, e27780, 2024, doi: 10.1016/j.heliyon.2024.e27780.
[52] O. Assogba, A. Bréard, and Y. Duroc, "A new low-cost compact antenna for the 2.45 and 5.8 GHz ISM bands," Appl. Sci., vol. 15, no. 4, p. 1912, 2025, doi: 10.3390/app15041912.
[53] H. Xing, X. Wang, Z. Gao, X. An, H. X. Zheng, M. Wang, and E. Li, "Efficient isolation of an MIMO antenna using defected ground structure," Electronics, vol. 9, no. 8, p. 1265, 2020, doi: 10.3390/electronics9081265.
[54] M. Ameen, O. Ahmad, and R. K. Chaudhary, "Wideband circularly-polarised high-gain diversity antenna loaded with metasurface reflector for small satellite applications," Electron. Lett., vol. 55, no. 15, pp. 829–831, 2019, doi: 10.1049/el.2019.1645.
[55] G. Das, A. Sharma, R. K. Gangwar, and M. S. Sharawi, "Triple-port, two-mode based two element cylindrical dielectric resonator antenna for MIMO applications," Microw. Opt. Technol. Lett., vol. 60, no. 6, pp. 1566–1573, 2018, doi: 10.1002/mop.31202.
[56] K. Sharma and G. P. Pandey, "Two port compact MIMO antenna for ISM band applications," Prog. Electromagn. Res. C, vol. 100, pp. 173–185, 2020, doi: 10.2528/PIERC20011504.
[57] E. Fritz-Andrade, A. Perez-Miguel, R. Gomez-Villanueva, et al., "Characteristic mode analysis applied to reduce the mutual coupling of a four-element patch MIMO antenna using a defected ground structure," IET Microw. Antennas Propag., vol. 14, no. 2, pp. 215–226, 2020, doi: 10.1049/iet-map.2019.0570.
[58] G. Varshney, R. Singh, V. S. Pandey, and R. S. Yaduvanshi, "Circularly polarized two-port MIMO dielectric resonator antenna," Prog. Electromagn. Res. M, vol. 91, pp. 19–28, 2020, doi: 10.2528/PIERM20011003.
[59] A. J. Alazemi and A. Iqbal, "A compact and wideband MIMO antenna for high-data-rate biomedical ingestible capsules," Sci. Rep., vol. 12, no. 1, p. 14290, 2022, doi: 10.1038/s41598-022-18468-2.
[60] M. N. Abbasi, A. Aziz, W. A. Malik, A. R. Chishti, and R. Hussain, "A simple and modular MIMO antenna system for closely spaced patch antennas," Microw. Opt. Technol. Lett., vol. 64, no. 7, pp. 1210–1216, 2022, doi: 10.1002/mop.33257.
[61] J. Kulkarni, R. K. Gangwar, and J. Anguera, "Broadband and compact circularly polarized MIMO antenna with concentric rings and oval slots for 5G application," IEEE Access, vol. 10, pp. 29925–29936, 2022, doi: 10.1109/ACCESS.2022.3157914.
[62] P. Sharma, R. N. Tiwari, P. Singh, and B. K. Kanaujia, "Dual-band trident shaped MIMO antenna with novel ground plane for 5G applications," AEU-Int. J. Electron. Commun., vol. 155, p. 154364, 2022, doi: 10.1016/j.aeue.2022.154364.
[63] Z. Du, X. Zhang, P. Qin, Y. Pu, and X. Xi, "Intercoupling suppression of very closely spaced MIMO antenna based on current cancellation method," IEEE Access, vol. 12, pp. 55103–55110, 2022, doi: 10.1109/ACCESS.2022.3224461.
[64] G. Reddy, N. M. Prasad, A. K. Dwivedi, et al., "Metasurface-loaded ceramic-based MIMO antenna with high isolation and circular polarization features," J. Electron. Mater., vol. 52, no. 2, pp. 1305–1313, 2023, doi: 10.1007/s11664-022-10088-w.
[65] V. Dhasarathan, T. K. Tran, J. Kulkarni, B. A. Garner, and Y. Li, "Mutual coupling reduction in dual-band MIMO antenna using parasitic dollar-shaped structure for modern wireless communication," IEEE Access, vol. 11, pp. 5617–

This article has license CC BY 4.0 https://creativecommons.org/licenses/by/4.0/

5628, 2023, doi: 10.1109/ACCESS.2023.3235761.
[66] P. Gupta, M. Bharti, and A. Kumar, "Two-element UWB antenna with multiple open slots in fountain-shaped ground for wearable and biomedical applications," MAPAN, vol. 38, no. 1, pp. 203–215, 2023, doi: 10.1007/s12647-022-00607-9.
[67] R. Rebbah, I. Messaoudene, M. Khelifi, B. Hammache, and T. A. Denidni, "Enhanced isolation of MIMO cavity antenna using substrate integrated waveguide technology," Microw. Opt. Technol. Lett., vol. 64, no. 2, pp. 331–337, 2022, doi: 10.1002/mop.33091.
[68] C. Wang, H. Wang, P. Wu, and M. Hou, "Dual-band closed-slot MIMO antenna for terminal wireless applications," IEEE Trans. Antennas Propag., vol. 70, no. 8, pp. 6514–6525, 2022, doi: 10.1109/TAP.2022.3161531.
[69] H. Ahmed, A. M. Ameen, A. Magdy, A. Nasser, and M. Abo-Zahhad, "A Sub-6GHz two-port crescent MIMO array antenna for 5G applications," Electronics, vol. 14, no. 3, p. 411, 2025, doi: 10.3390/electronics14030411.
[70] A. Gupta, M. Aljaidi, S. Bansal, R. E. Al Mamlook, V. Kumar, A. Aljohani, S. Aljohani, and M. K. Singla, "Design analysis and performance enhancement of a 2-element MIMO skin-implantable antenna for IoT-based health monitoring devices," PLoS One, vol. 19, no. 12, e0311753, 2024, doi: 10.1371/journal.pone.0311753.
[71] W. A. Neamah, H. M. Al Sabbagh, and H. Al-Rizzo, "A compact two-element linearly and orthogonal circularly polarized MIMO antenna system for 5G cellular and WLAN/Wi-Fi 6E application," IEEE Access, vol. 11, pp. 96879–96891, 2023, doi: 10.1109/ACCESS.2023.3312122.
[72] M. N. Abbasi, A. Aziz, K. A. Aljaloud, A. R. Chishti, Y. T. Aladadi, and R. Hussain, "A close proximity 2-element MIMO antenna using optically transparent wired-metal mesh and polyethylene terephthalate material," IEEE Access, vol. 11, pp. 78811–78819, 2023, doi: 10.1109/ACCESS.2023.3298568.

Accepted Manuscript: Author Version

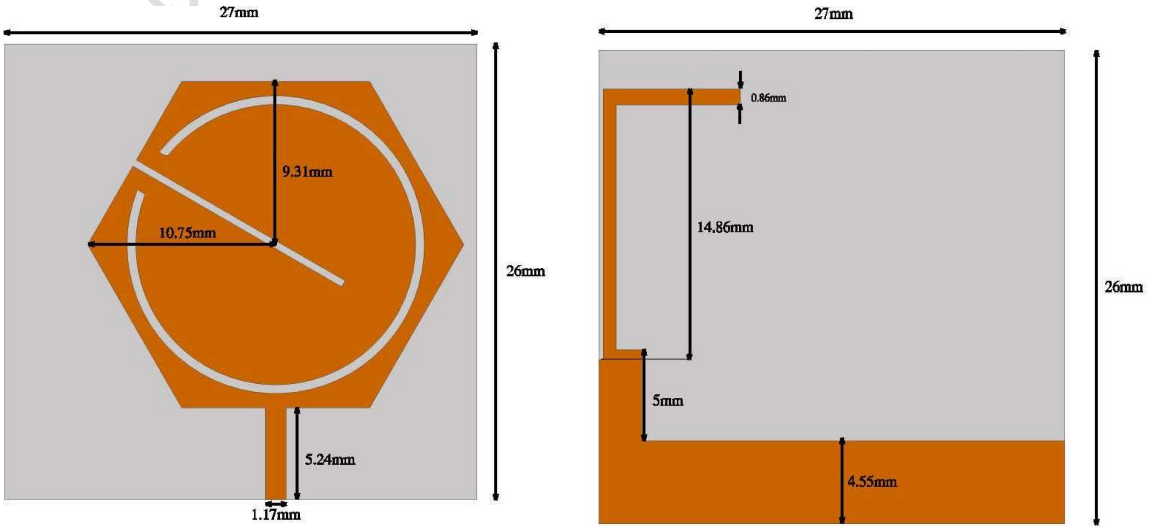

This article has license CC BY 4.0 https://creativecommons.org/licenses/by/4.0/

(a) (b)

Fig. 1. The Microstrip antenna, (a) top view, (b) bottom view.

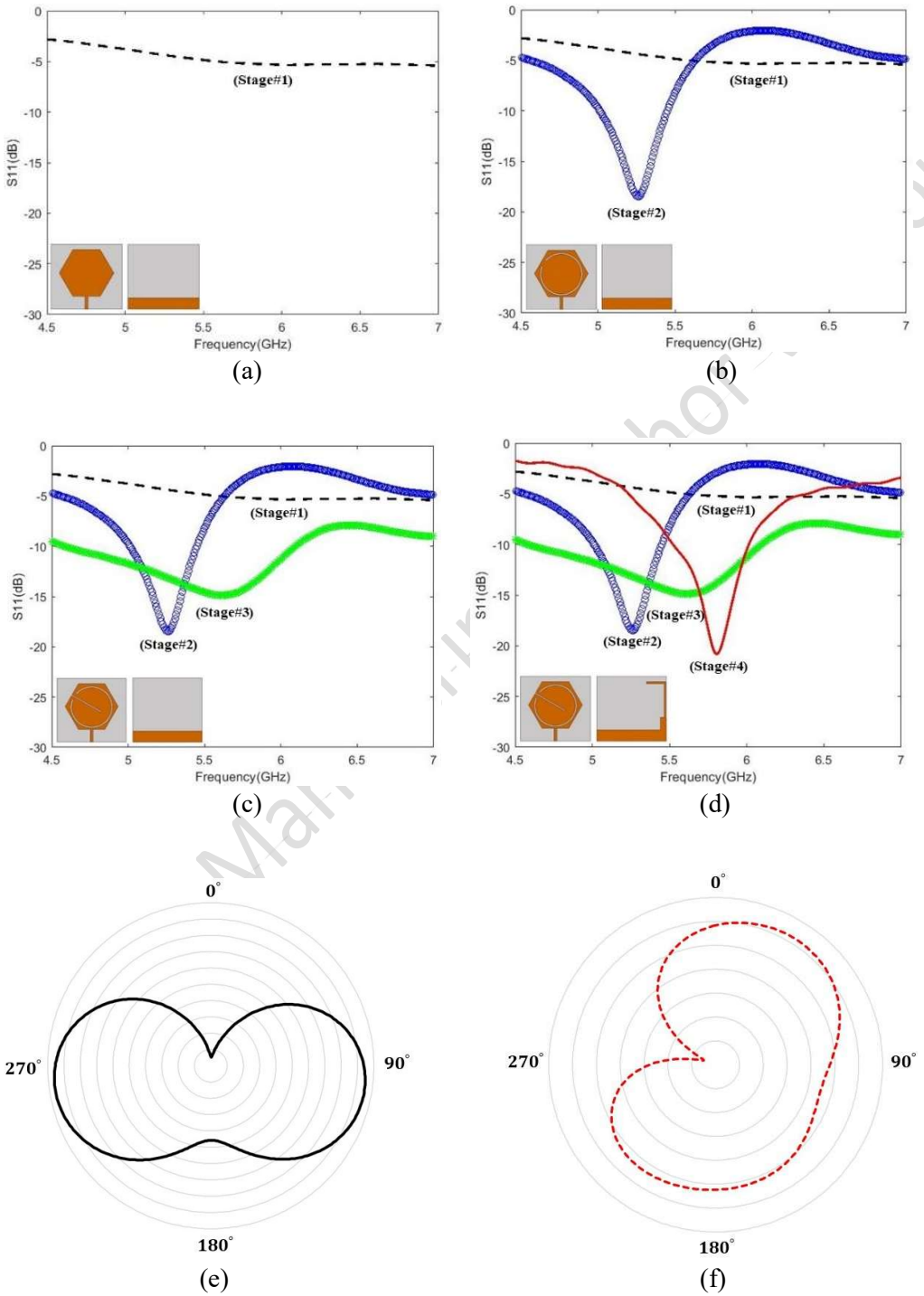

Fig. 2. The single-element antenna design steps with related S11 diagram (a) step#1, (b) step#2, (c) step#3, (d) step#4, simulated far-field pattern at 5.8 GHz (e) H-plane (f) E-plane.

This article has license CC BY 4.0 https://creativecommons.org/licenses/by/4.0/

Accepted manuscript (author version)

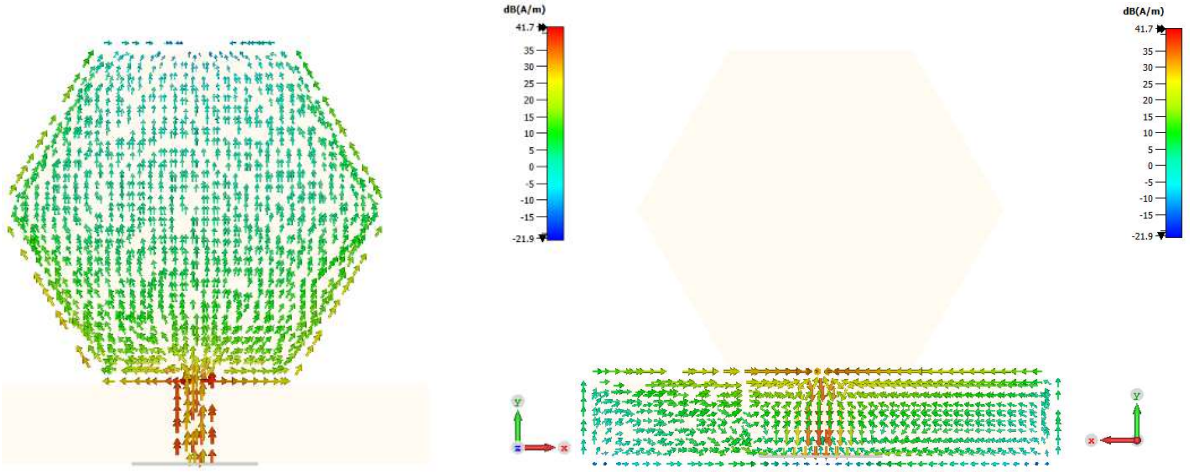

(a)

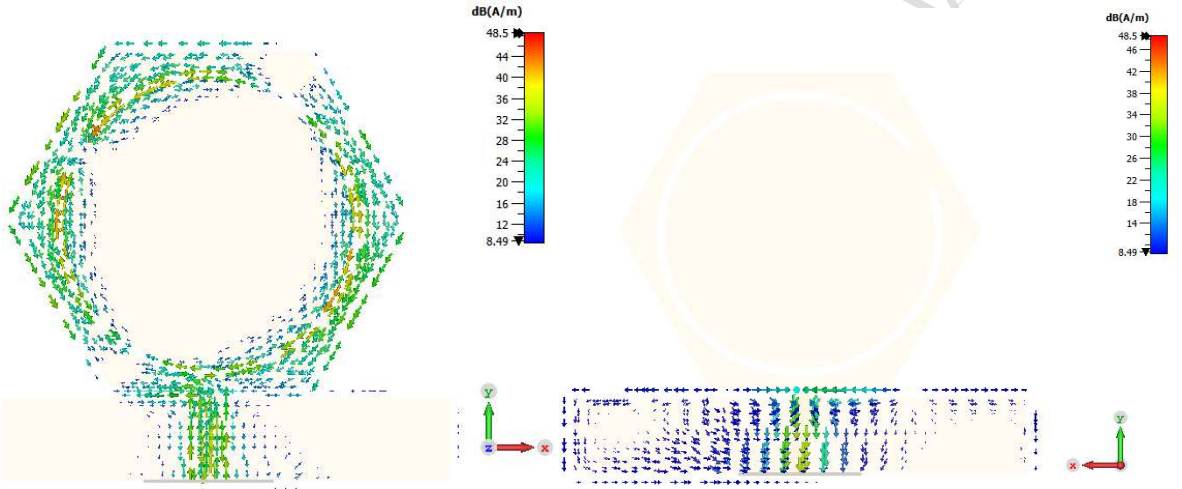

(b)

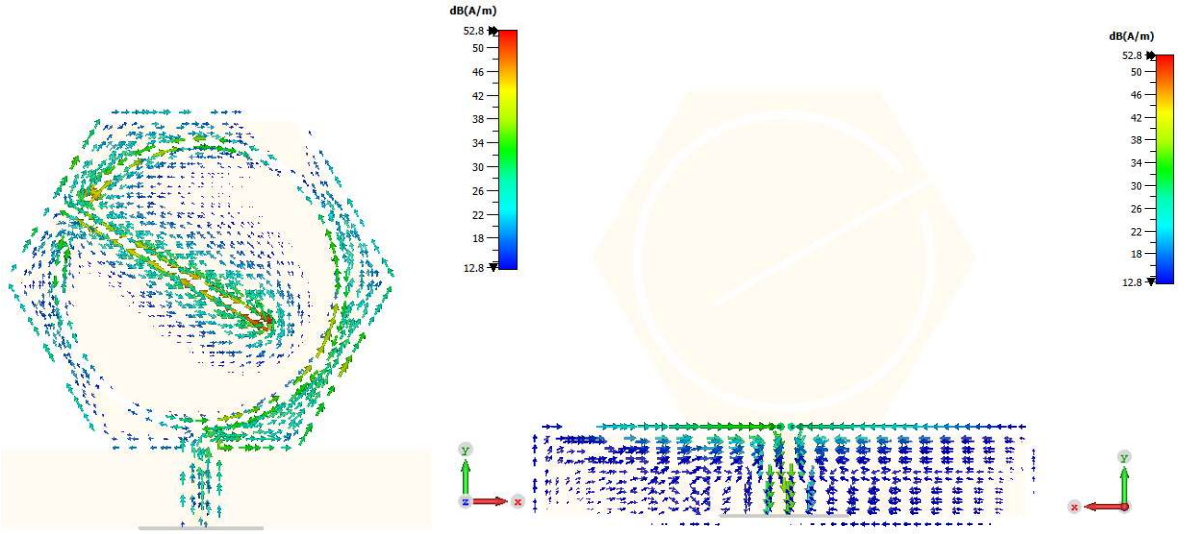

(c)

This article has license CC BY 4.0 https://creativecommons.org/licenses/by/4.0/

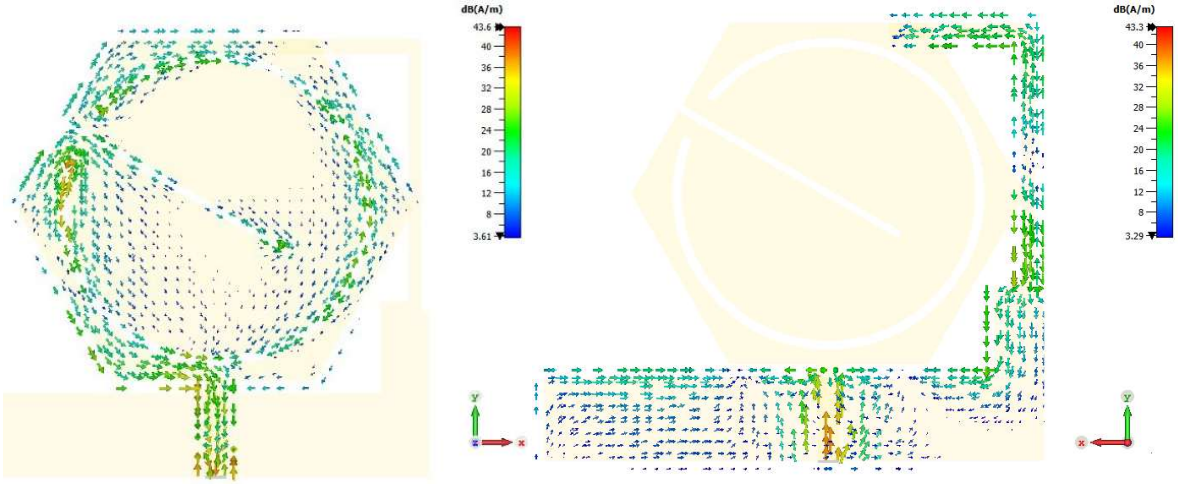

(d)

Fig. 3. Distribution of surface current at 5.8 GHz (a) step#1, (b) step#2, (c) step#3, (d) step#4.

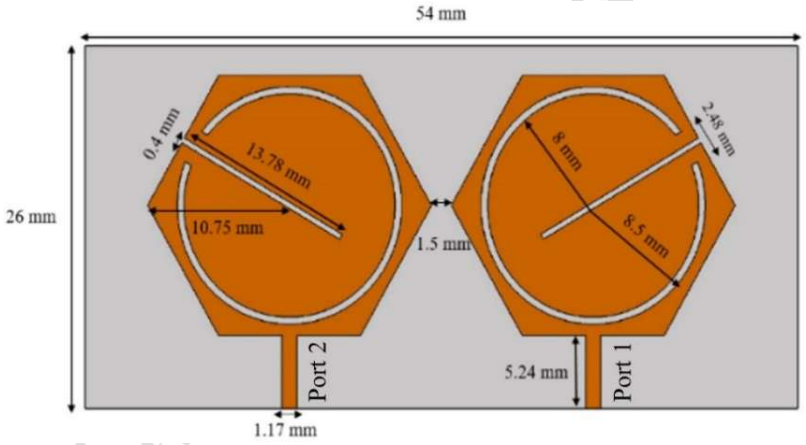

(a)

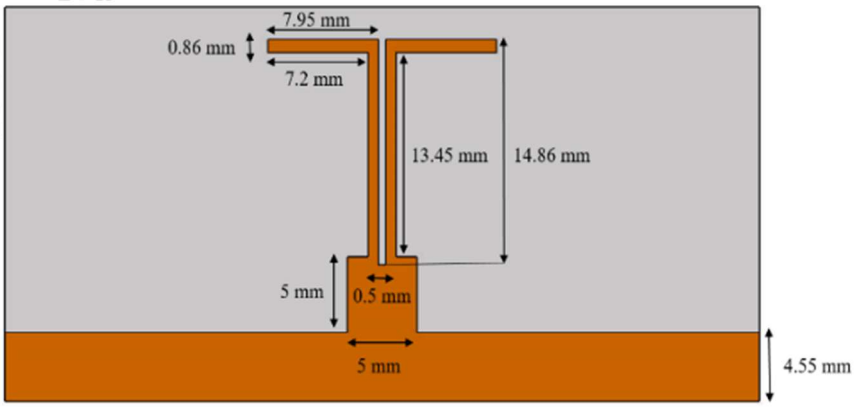

(b)

Fig. 4. The proposed microstrip MIMO array with designed details: (a) top view, (b) bottom view.

This article has license CC BY 4.0 https://creativecommons.org/licenses/by/4.0/

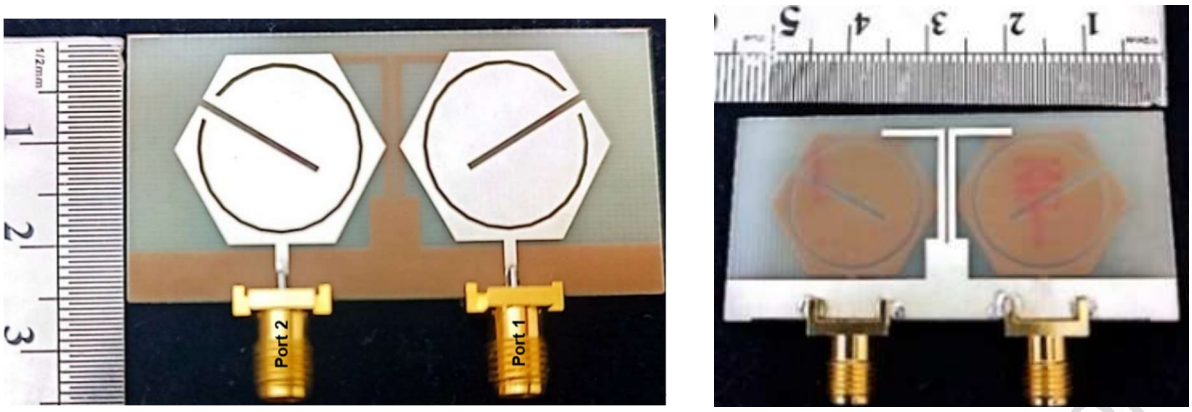

(a) (b)

Fig. 5. The photographs of fabricated prototype microstrip MIMO array: (a) top photo, (b) bottom photo.

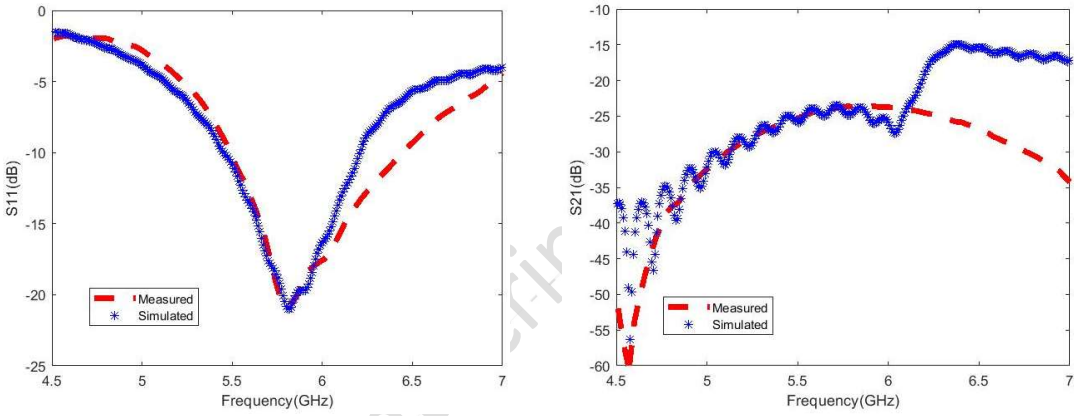

(a) (b)

Fig. 6. Measured and simulated (a) S11 and (b) S21 parameters of MIMO antenna.

Accepted Manuscript (author version)

This article has license CC BY 4.0 https://creativecommons.org/licenses/by/4.0/

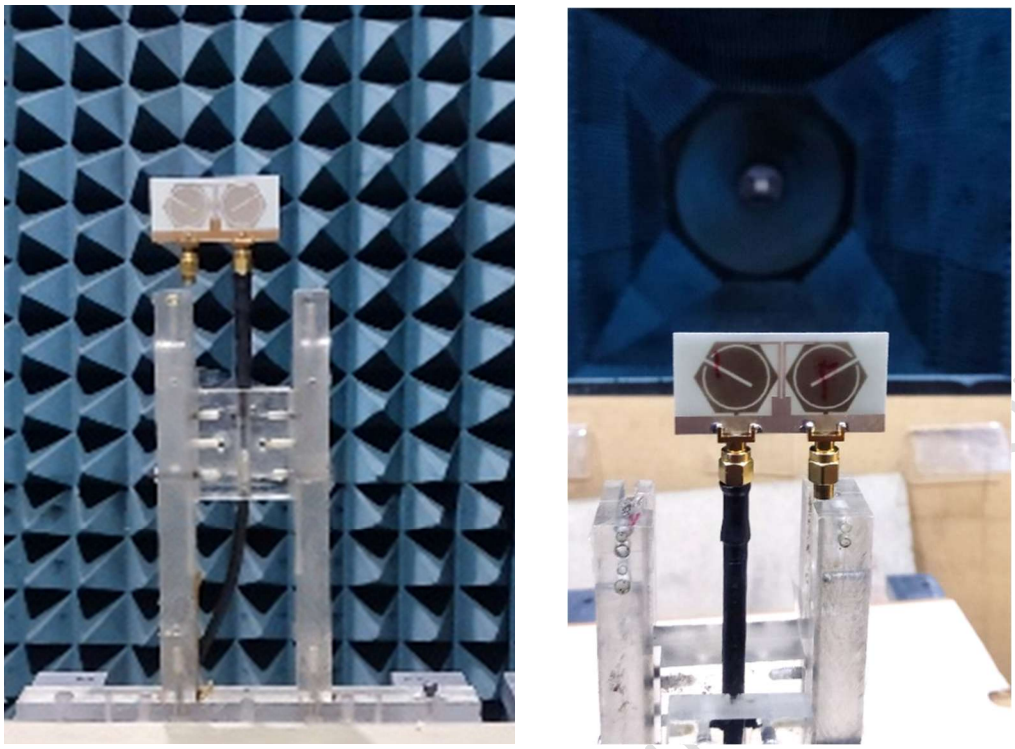

Fig. 7. The photograph of the fabricated prototypes of the MIMO antenna under test in anechoic chamber.

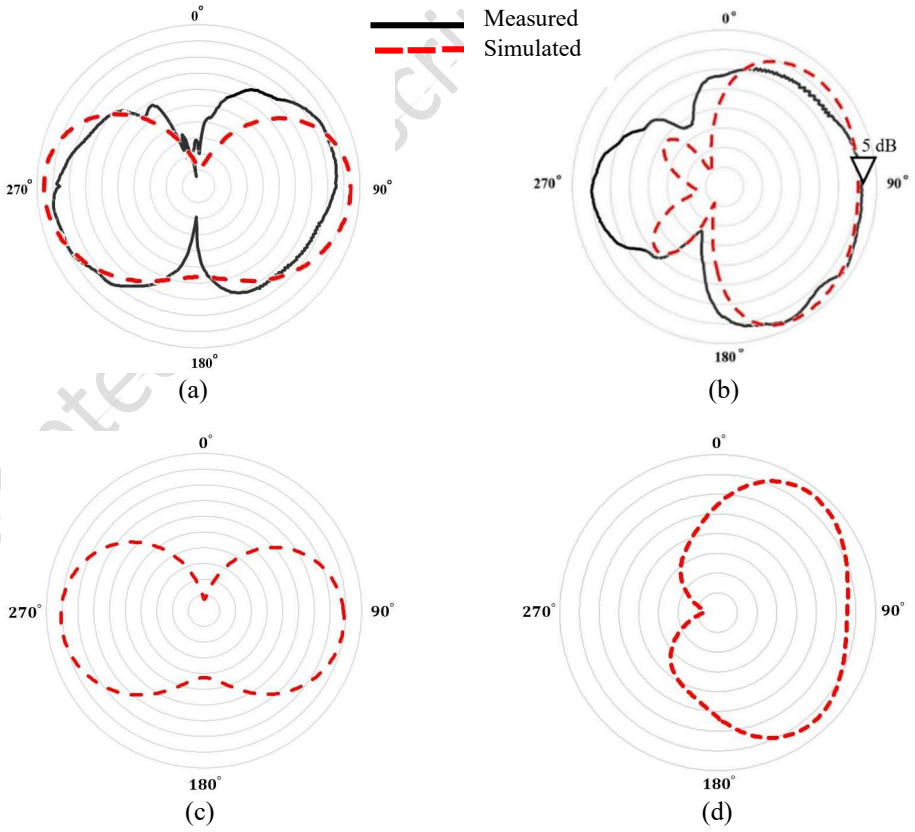

This article has license CC BY 4.0 https://creativecommons.org/licenses/by/4.0/

Accepted manuscript (author version)

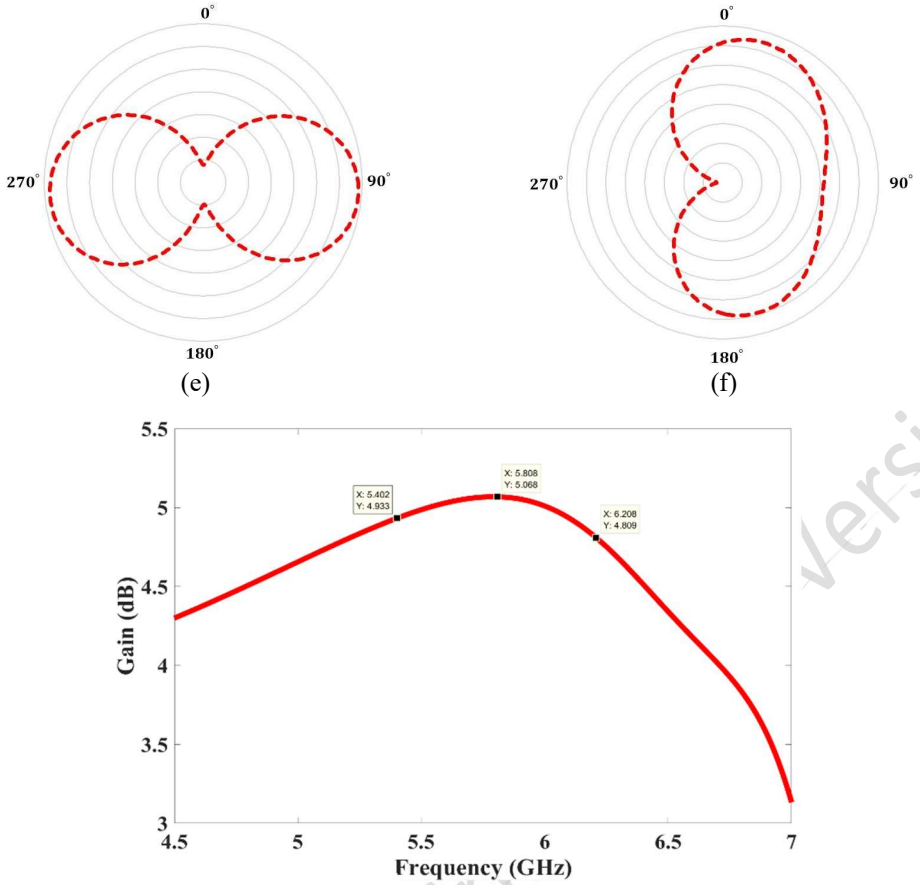

Fig. 8. Measured and simulated (a) H-plane, (b) E-plane far-field pattern at 5.8 GHz, simulated of far-field pattern at 5.4 GHz (c) H-plane, (d) E-plane, and simulated of far-field pattern at 6.2 GHz (e) H-plane, (f) E-plane, (g) Diagram of antenna gain across the frequency range covered.

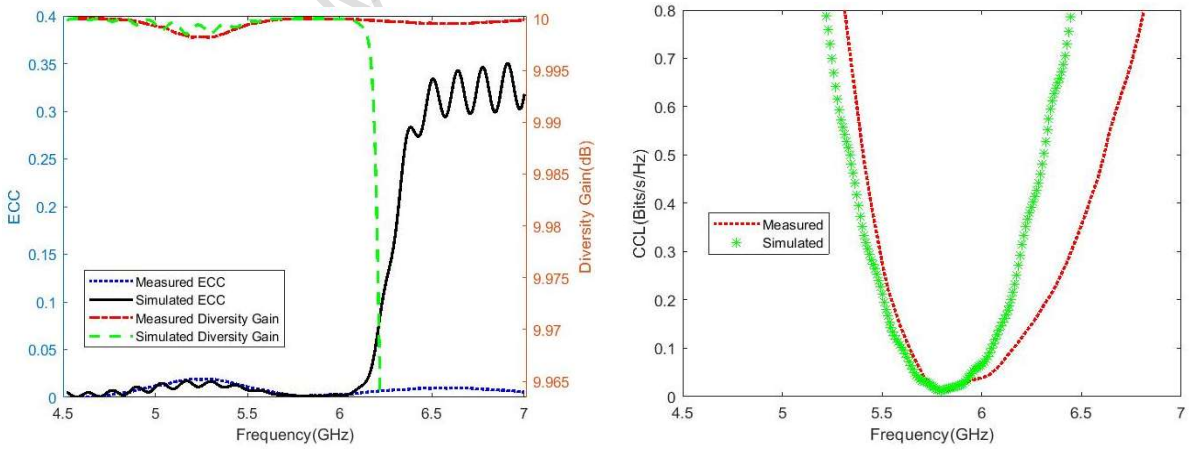

This article has license CC BY 4.0 https://creativecommons.org/licenses/by/4.0/

Accepted manuscript (author version)

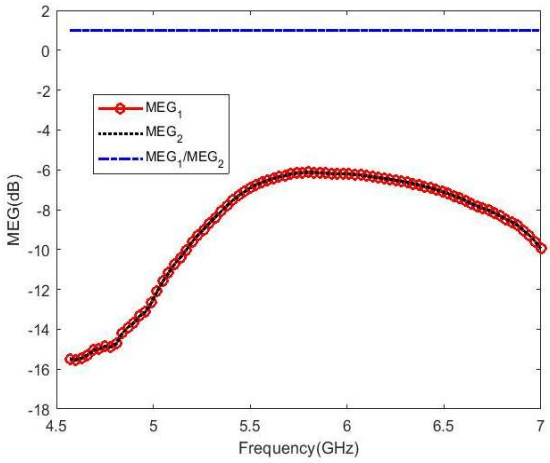

(c)

Fig. 9. The proposed MIMO antenna diversity parameter (a) Measured/ simulated DG and ECC, (b) Measured/ simulated CCL, (c) Simulated MEGs.

Accepted Manuscript: Author Version

This article has license CC BY 4.0 https://creativecommons.org/licenses/by/4.0/

Accepted manuscript (author version)

Table 1. Dimensions of the patch antenna.

	Dielectric constant of substrate ε_r	Thickness of substrate (mm)	Effective dielectric constant ε_{ff}	Patch Width (mm)	Patch Length (mm)	Extended incremental length ΔL (mm)
Original Value (Equations (1-5))	3.38	0.508	3.21	17.48	13.93	0.245
Modified Values (CST Microwave Studio)	3.38	0.508	3.24	21.5	18.62	0.248

Accepted Manuscript: Author Version

This article has license CC BY 4.0 https://creativecommons.org/licenses/by/4.0/

Accepted manuscript (author version)

Table 2 Performance comparisons between different parameters of the proposed microstrip MIMO antenna with previous works.

Ref.	Frequency (GHz)	Bandwidth % (GHz)	Dimension (λ^3)	Gain (dB)	Efficiency (%)	Isolation (dB)	Application(s)
[8], 2022	2.4 3.5 5.5	8 (2.28–2.47) 11 (3.34–3.73) 38 (4.57–6.75)	0.56 × 0.36 × 0.018	1.3 2.9 4.3	–	20	ISM, 5G, WLAN
[42], 2021	2.4 6.5	87 (3–7.7)	0.37 × 0.25 × 0.006	3	78	20	Wireless
[43], 2021	3.7	24 (3.3– 4.2)	0.45 × 0.36 × 0.009	2.5	95	15	5G
[53], 2020	5.8	2 (5.72–5.89)	1.07 × 0.87 × 0.029	5.36	–	20.19	Wireless
[54], 2019	2.6	29 (2.16–2.92)	0.34 × 0.19 × 0.013	7.02	82.1	14.5	Small Satellite
[55], 2018	5.5	11 (5.25–5.92)	1.10 × 0.73 × 0.157	5	90	20	WLAN
[56], 2020	2.46	2.83 (2.43–2.5)	0.76 × 0.30 × 0.012	4.25	77.81	24.67	WLAN
[57], 2020	5.8	3.44 (5.7–5.9)	1.06 × 1.06 × 0.309	5.3	84	32	WLAN, LTE
[58], 2020	6.44	35 (5.71–8.2)	1.70 × 1.70 × 0.106	3.8	80	15	C-band
[59], 2022	2.45	25 (2.15–2.77)	0.04 × 0.03×0.00096	-22.7	–	30.1	Wireless capsule
[60], 2022	6	3 (5.9–6.1)	0.80 × 0.64 × 0.02	5.2	73	40	5G
[61], 2022	4	46 (3.12–5)	0.33 × 0.26 × 0.021	2.5	70	18.5	5G
[62], 2022	3.38 4.78	18.3 (2.99–3.61) 8.1 (4.53–4.92)	0.68 × 0.28 × 0.016	3.05 3.76	74.46 84.93	25 16	5G
[63], 2023	5.37	2 (5.3–5.46)	0.68 × 0.56 × 0.017	4.54	74	51.5	–
[64], 2023	5.4	10.8 (5.25–5.85)	1.43 × 0.89 × 0.014	6.5	90	25	WLAN
[65], 2023	2.5 4.5	6 (2.40–2.57) 57 (3.85–6.96)	0.37 × 0.25 × 0.006	2.65	70	15	5G, Wi-Fi
[66], 2023	3.7–7.7	112 (2.9–10.4)	0.43 × 0.30 × 0.019	5	90	20	IoT, Wearable
[67], 2022	5.8	4 (5.65–5.9)	0.48 × 0.99 × 0.03	5.6	93	17-30	WLAN
[68], 2022	2.4 5.56	12.7 (2.2–2.5) 10.7 (5.2–5.8)	1.40 × 0.80 × 0.012	–	28 16.2	20	Wi-Fi
[69], 2025	3.5 5.8	(3.01-6.5)	0.77 × 0.77 × 0.018	7.66 7.74	71.5	20	5G, WiMAX
[70], 2024	2.4	20.8 (2.2-2.7)	0.128 × 0.048×0.002	2.3	5.41	34	IoT
[71], 2023	3.5 6	35.7 (3.45 – 4.7) 36.6 (5.6-7.8)	0.6 × 0.41 × 0.021	1 3.8	87 85	17 26	5G, WLAN
[72], 2023	5.8	3.4 (5.7-5.9)	0.65 × 0.56	3.55	65	25	5G, IoT
Propoesd	5.8	13.79 (5.4–6.2)	1.04 × 0.50 × 0.0098	5	95	22	ISM, IoT

Accepted Manuscript: Author Version

This article has license CC BY 4.0 https://creativecommons.org/licenses/by/4.0/